Physical Mechanisms Controlling the Offshore Propagation of Convection in the Tropics: 2. Influence of Topography

David Coppin, Gilles Bellon

JAMES | Journal of Advances in Modeling Earth Systems

RESEARCH ARTICLE
10.1029/2019MS001794

This article is a companion to Coppin & Bellon (2019), https://doi.org/10.1029/2019MS001793.

Key Points:
- Clouds clinging to topography weaken nocturnal offshore propagation of convection
- The same mechanisms trigger offshore convection with flat island and with topography
- Valley breeze effect reinforces the propagation speed of the land breeze

Correspondence to:
D. Coppin,
david.ad.coppin@gmail.com

Citation:
Coppin, D., & Bellon, G. (2019). Physical mechanisms controlling the offshore propagation of convection in the tropics: 2. Influence of topography. *Journal of Advances in Modeling Earth Systems*, *11*, 3251–3264. https://doi.org/10.1029/2019MS001794

Received 28 JUN 2019
Accepted 31 AUG 2019
Accepted article online 6 SEP 2019
Published online 25 OCT 2019

Physical Mechanisms Controlling the Offshore Propagation of Convection in the Tropics: 2. Influence of Topography

David Coppin[1] **and Gilles Bellon**[1]

[1]Department of Physics, University of Auckland, Auckland, New Zealand

Abstract A set of idealized convection-permitting simulations is performed to investigate the influence of topography on the physical mechanisms responsible for the nocturnal offshore propagation of convection around tropical islands. All simulations have an idealized island in the middle of a long channel oceanic domain, with constant sea surface temperature and without rotation. To diagnose the impact of topography, we compare a flat island simulation with two simulations with mountain ranges of different shapes. The topography over the island has a strong impact on the diurnal cycle of convection as clouds tend to remain all day over the highest topography. This weakens the diurnal cycle and the land breeze front and triggers a comparatively less frequent long-distance offshore propagation of convection. As in the flat simulation, the distance of offshore propagation is particularly sensitive to humidity and temperature at the top of the boundary layer. A shallow circulation that is asymmetric with respect to the island influences the boundary layer top humidity and can favor propagation on one side of the island or the other. These results mimic cloud and precipitation patterns observed prior to the Madden-Julian Oscillation propagation over the Maritime Continent. The shape of the topography does not seem to influence the offshore propagation of convection significantly except for mountain-valley breezes that reinforce the land breeze and the establishment of the asymmetric shallow circulation.

Plain Language Summary In Part I of this paper, we looked at the mechanisms controlling the offshore propagation of convection around an idealized flat tropical island. But tropical islands generally have high topography reaching thousands of meters over Papua New Guinea, Borneo, and Sumatra. The impact of topography is investigated using the same framework as before but with a mountain range on the island. We test two different shapes to investigate valley breeze effects and the dependence on the mountain shape: one is a simple ridge and the other has a peak and a pass. The presence of a mountain range strongly affects the offshore propagation of convection as clouds tend to stay above the highest topography at night, which weakens the land breeze. Gravity waves triggering convection far from the coast are present but only for days when clouds move away from the coast at night. The valley is found to reinforce the land breeze and, more surprisingly, allows the development of asymmetric offshore convection relative to the island. This asymmetry, also found with the flat island simulation, is responsible for the advection of a dry anomaly that forces convection to stay close to the coast more frequently.

1. Introduction

Part I of this paper (Coppin & Bellon, 2019) describes the physical mechanisms controlling the offshore propagation of convection around an idealized flat tropical island. In this simulation, a sea breeze systematically develops in the morning, followed by convection in mid afternoon, early evening, and an offshore propagation of convection over the surrounding ocean at night. This diurnal cycle of island convection is realistic (Mori et al., 2004; J.-H. Qian, 2008; Yang & Slingo, 2001); in particular, the timing of convection triggering over the island is well simulated, while many models tend to simulate it too early (Neale & Slingo, 2003; Peatman et al., 2015; J.-H. Qian, 2008).

In Part I, we identify two main phenomena in the control of nocturnal offshore propagation of convection over the ocean for a flat island. A land breeze propagates at an average speed of 3–4 m/s, similar to values found in observations (Mori et al., 2011; Yokoi et al., 2017) and other high-resolution modeling studies (Hassim et al., 2016; Love et al., 2011; Vincent & Lane, 2016). This propagation speed depends on the large-scale wind speed, mostly modulated by the presence of convection triggered earlier and further

offshore by gravity waves when the environmental conditions are favorable. In our model, two gravity wave modes stand out: the first and second baroclinic modes, propagating at 30 and 20 m/s, respectively. The first baroclinic mode is reminiscent of gravity waves generated by the diurnal heating over islands found in Love et al. (2011). The second baroclinic mode resembles the gravity waves triggering offshore convection in several modeling studies (Hassim et al., 2016; Mapes et al., 2003; Vincent & Lane, 2016), even though it is slightly faster in our model.

Topography also plays a crucial role in controlling the diurnal cycle of precipitation over tropical islands. Early work showed that precipitation is enhanced by upslope winds over islands with a mountain range (J.-H. Qian, 2008; Yang & Slingo, 2001). Depending on the direction of the wind, topography can enhance convection and its offshore propagation on one side of the mountain range and suppress it on the other side (Ichikawa & Yasunari, 2007, 2008; Qian et al., 2013). This blocking effect of the mountain range is also found to strengthen the sea breeze (T. Qian et al., 2012). In that study, the sea breeze is modeled as the response to an oscillating heat source over a flat land or an inland plateau. When topography is added, the partial blocking of the sea breeze traps cool air at the base of the plateau near the end of the heating cycle. This air is cooled further during the night and generates a stronger cold pool that leads to a stronger land breeze as well as a faster propagation. Experiments show that the strength of the land breeze increases with the terrain height, at least for moderate heights. Elevated terrain also pushes the diurnal heating upward into the stratified layers of the surrounding atmosphere, generating gravity waves that help trigger offshore convection (Mapes et al., 2003). When topography is more realistic than an idealized elevated plateau, additional effects occur. During daytime, sea breezes converge in valleys, enhancing and focusing convection over the mountains (J.-H. Qian, 2008). At night, downslope winds also converge in valleys and reinforce the land breeze (Vincent & Lane, 2016).

Local processes associated with the diurnal cycle can interact or compete with variability at larger scales. The arrival of the Madden-Julian Oscillation (MJO; R. A. Madden & Julian, 1971; R. A. Madden and Julian, 1972, 1994; Zhang, 2005) over the Maritime Continent is a good example of such interaction. One or two phases before the main envelope of the MJO reaches the Maritime Continent; the diurnal cycle over the island is enhanced, followed by an enhancement of the diurnal cycle over the surrounding oceans in regions of offshore-propagating convection (Peatman et al., 2014). Later on during the active phase of the MJO over the Maritime Continent, the MJO propagation can be hindered by a strong diurnal cycle over islands because it competes with large-scale convection over the ocean for moisture supply: the moisture convergence over islands due to sea breezes dries the oceanic regions (Hagos et al., 2016). Hence, understanding how topography affects the offshore propagation of convection may be crucial to better simulate the propagation or blocking of the MJO over the Maritime Continent.

The aim of this study is to analyze how topography impacts the nocturnal offshore propagation around an idealized tropical island. Section 2 presents the simulations with topography and the setup used. Section 3 analyzes the similarities and differences observed between the simulations with topography and the simulation with a flat island from Part I. Section 4 focuses on the changes resulting from different shapes of mountain ranges.

2. Methods

Similar to Part I, we run the mesoscale nonhydrostatic atmospheric model Meso-NH version 5.3.1 (Lafore et al., 1998; Lac et al., 2018) coupled with the SURFEX model (Masson et al., 2013) over land, with the same Radiative Convective Equilibrium setup: long doubly periodic channel, 2,048 km × 128 km in x and y directions, respectively, with 47 stretched vertical levels and a top at 25 km, an island of 128 km× 128 km in the middle of the domain, no Coriolis force, and no large-scale wind forcing. Similar to Part I, even though we do not impose a wind forcing, an overturning large-scale circulation develops due to the maintenance of convection over and around the island and low-level winds associated with this circulation converge over the island. We call these winds large-scale winds hereafter.

Two different mountain shapes are tested and illustrated in Figure 1: one with a ridge (simulation Ridge) and one with a peak and a pass (simulation Peak). We will compare these simulations to the simulation without topography analyzed in Part I (simulation Flat).

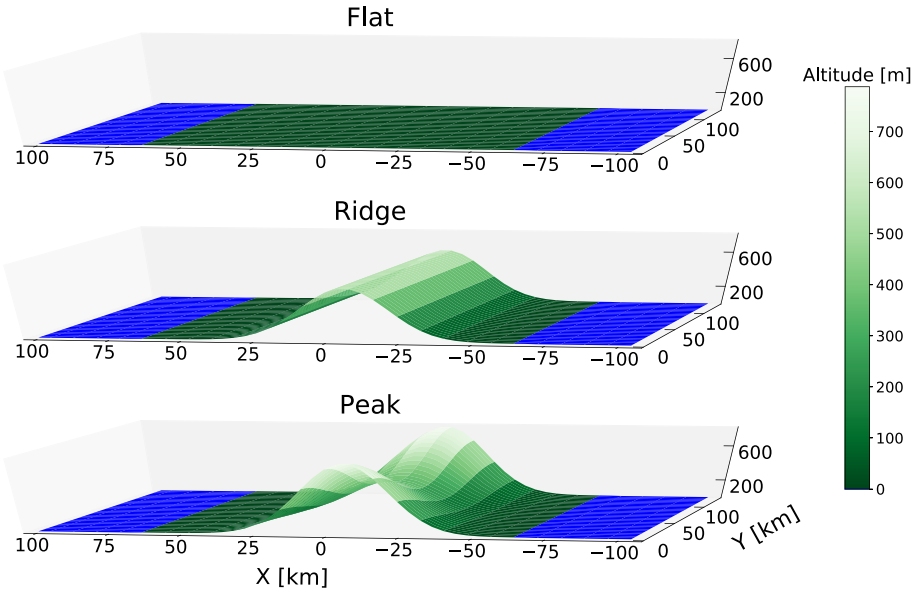

Figure 1. Topography for simulations Flat, Ridge, and Peak. Only 200 km of the domain around the island is shown.

More specifically, in simulation Ridge, the topography varies only in direction x and has a Gaussian shape:

$$h_{\text{ridge}}(x,y) = He^{-\frac{(x-x_0)^2}{2\sigma_x^2}} \tag{1}$$

where H=600 m is the altitude of the ridge, x_0 correspond to the center of the island, and the standard deviation σ_x=15. The maximum altitude of the ridge is chosen to be representative of mountain plateau found over Sumatra, Java, and Borneo (even though the peaks on all these islands are much higher).

Topography in simulation Peak is a combination of the same Gaussian distribution in the x direction and a sinus in the y direction, which creates a valley, a pass at 400 m, and a peak at 800 m:

$$h_{\text{peak}}(x,y) = He^{-\frac{(x-x_0)^2}{2\sigma_x^2}}\left(1-\frac{1}{3}\cos\left(2\pi\frac{y}{L_y}\right)\right) \tag{2}$$

with L_y=128 km the width of the channel.

With these definitions, both mountains have the same average altitude for each point in the x direction. At the crest, this altitude corresponds to a Froude number below 1, indicating that these mountain ranges do not block the large-scale flow associated with the lower branch of the overturning large-scale circulation, which we wanted to avoid. Contrasting the two simulations will shed some light on whether mountain-valley winds reinforce convection and the land breeze and see if the geography of the island influences the wind fields themselves. Both simulations are performed for 250 days, and they reach a stationary state after about 40 days.

In most figures showing composites (Figures 2, 4, and 7–11), variables are composited a function of the distance $|x-x_0|$ to the center of the island, including both sides of the island, as in Part I, to increase sampling. If not specified otherwise, the composites are averages over the last 200 days of simulation and over direction y.

3. Comparison With Flat Island Simulation

In this section, we investigate the effect of island mountain ranges by analyzing the similarities and differences between simulation Flat and both simulations with topography.

3.1. Global Composites

Both simulations with topography have the same sea breeze in the morning to early afternoon followed by convection over the island in early evening and an offshore propagation of convection later at night similar to simulation Flat (Figure 2).

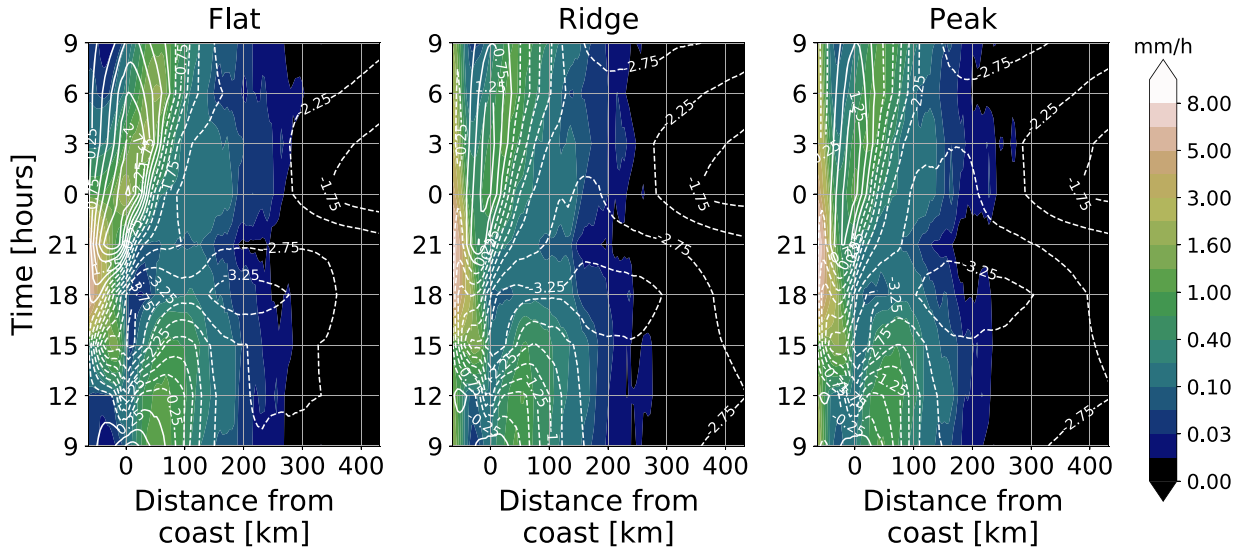

Figure 2. Diurnal composite of precipitation (shading) and wind at 75 m (contours, m/s) averaged over 200 days and direction *y* for (a) simulation Flat, (b) simulation Ridge, and (c) simulation Peak. The composite considers both sides of the island and is built so that the left of the figure is the center of the island. All distances are relative to the coast (0 mark).

Topography decreases the maximum distance of propagation in both simulations, defined as the point furthest from the coast where precipitation exceeds 0.33 mm/hr at least once in 24 hr. As in Part I, both sides of the island are considered independent to increase the sampling size. The mean distance of propagation is 112 and 100 km for simulations Ridge and Peak, respectively (compared to 141 km for simulation Flat). Both simulations with topography have a lot more instances of convection staying over the island or very close to it all day long and fewer cases of very long propagation (Figure 3).

The shorter propagation of convection in the simulations with topography is associated with a much weaker offshore land breeze than in the flat simulation (1 vs. 3 m/s in Figures 2b and 2c). The same budget analysis for wind and temperature as we presented in Part I for simulation Flat (see Figure 7 in Part I) indicates that this is nonetheless the signature of a land breeze (not shown). This difference in the land breeze speed does not result from the large-scale overturning circulation which is almost identical at 200 km from the coast in all three simulations (Figure 2), even though the daily profile of wind shows a slightly stronger onshore wind within 200 km from the coast in simulations with topography (Figure 4).

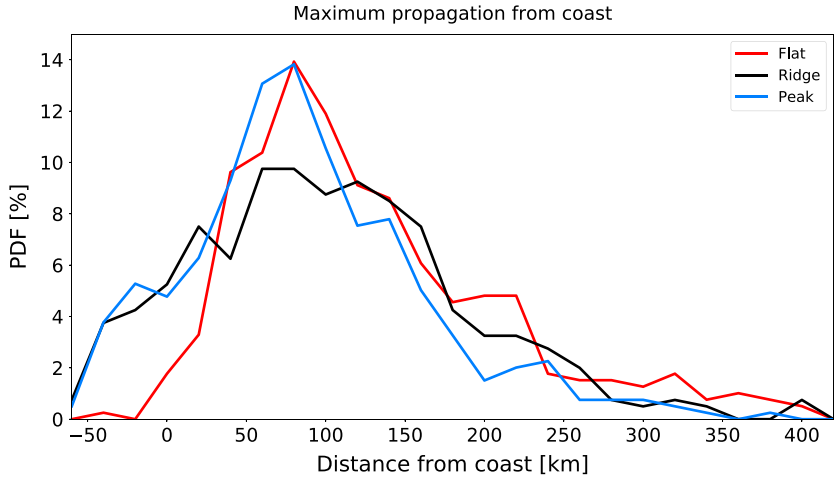

Figure 3. Probability density function of the maximum distance of propagation for simulations Flat (red line), Ridge (black line), and Peak (blue line). PDF = probability density function.

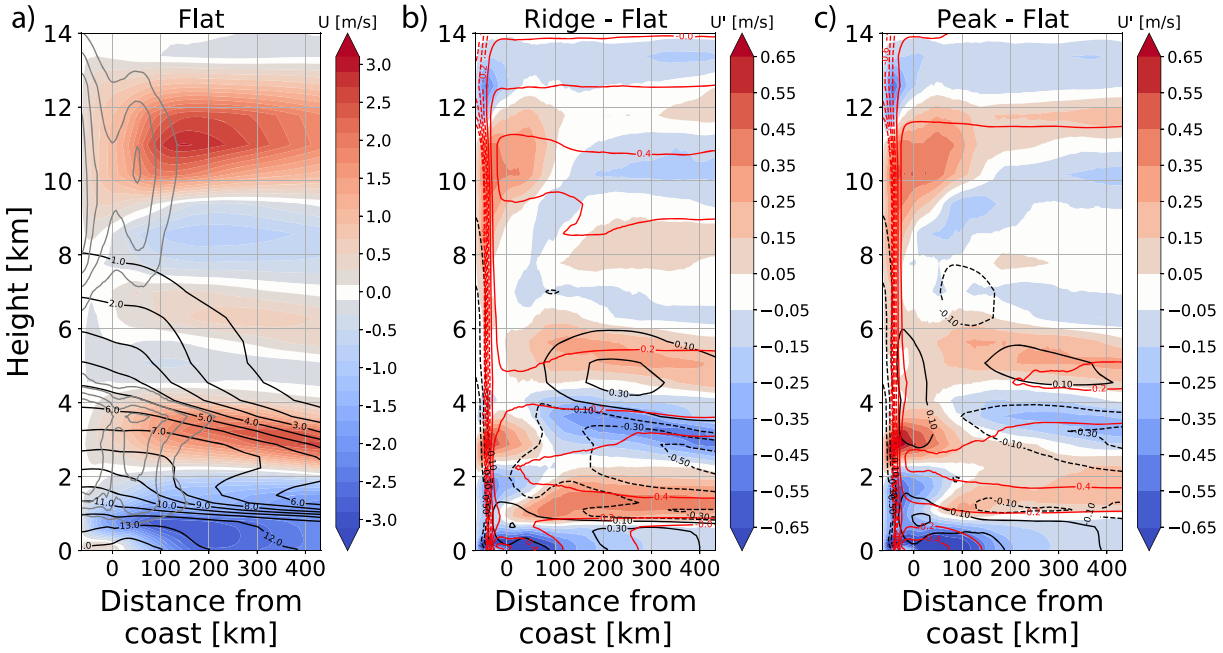

Figure 4. (a) Mean profile of zonal wind (shading), specific humidity (black contours, every g/kg) and specific cloud condensate (gray contours, every 10^{-5} kg/kg) in simulation Flat. (b) Differences in zonal wind (shading), specific humidity (black contours, every 2×10^{-1} g/kg), and temperature (red contours, every 10^{-1} K) between simulations Ridge and Flat. (c) Same as (b) between simulations Peak and Flat. Averages are calculated over 200 days and direction *y*.

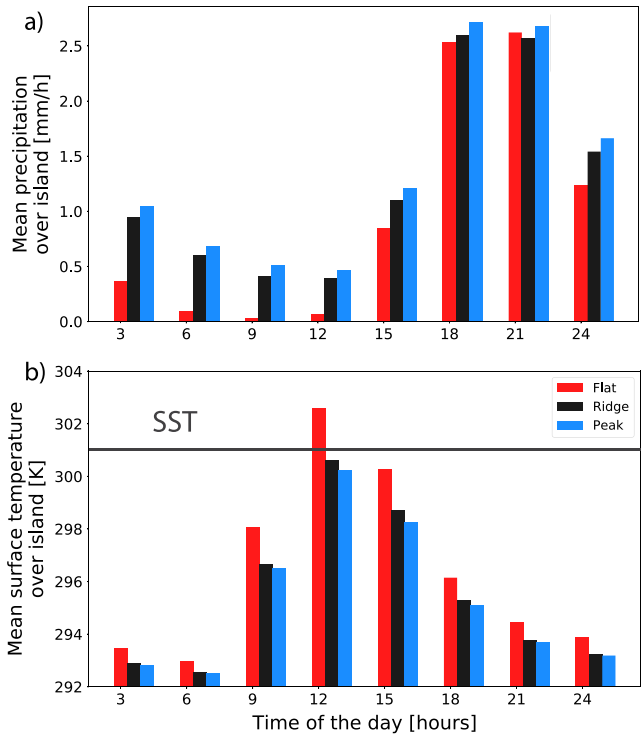

Figure 5. Diurnal histograms of (a) precipitation and (b) surface temperature over the island for simulations Flat (red line), Ridge (black line), and Peak (blue line). SST = sea surface temperature.

Figure 4 generally indicates that the mean circulation is stronger in the vicinity of the island (within 100 km from the coast) with more inflow in the boundary layer and more outflow in the lower troposphere (2–4 km) and the upper troposphere (9–12 km). Convection is also more localized above the mountain range in simulations Ridge and Peak. The temperature anomalies (red contours) show that the atmosphere is slightly more stable in these simulations except above the mountain range. Even though they also have a shallow circulation between the top of the boundary layer and 4 km, this circulation is weaker in simulations Peak and Ridge away from the island, the latter having an even more reduced circulation. Both simulations present a small drying of the lower troposphere far from the coast and a moister boundary layer, which can be interpreted as a decrease in shallow and midlevel convection. Again, this pattern is more intense in Ridge than in Peak, with some modulation due to advection by the moist outflows from the island.

The main difference between simulations with topography and simulation Flat is the persistence of precipitation over the island at night and in the morning (Figure 2). This difference is clearly visible when we compare averages over the whole island (Figure 5a).

The increased precipitation is associated with a larger cloud amount (contours in Figure 6), especially over the high topography.

Figure 6 also shows the effect of topography on surface temperature. The average height of the simulations with topography is 172 m, which results in an approximately 1.3 K lower surface temperature averaged over the island. The decrease of temperature with height is particularly visible over the topography (Figure 6). Near the coast where the height is the same in the three simulations, the temperature behaves similarly, with a diurnal warming up to 302 K. But on average over the island, the islands with

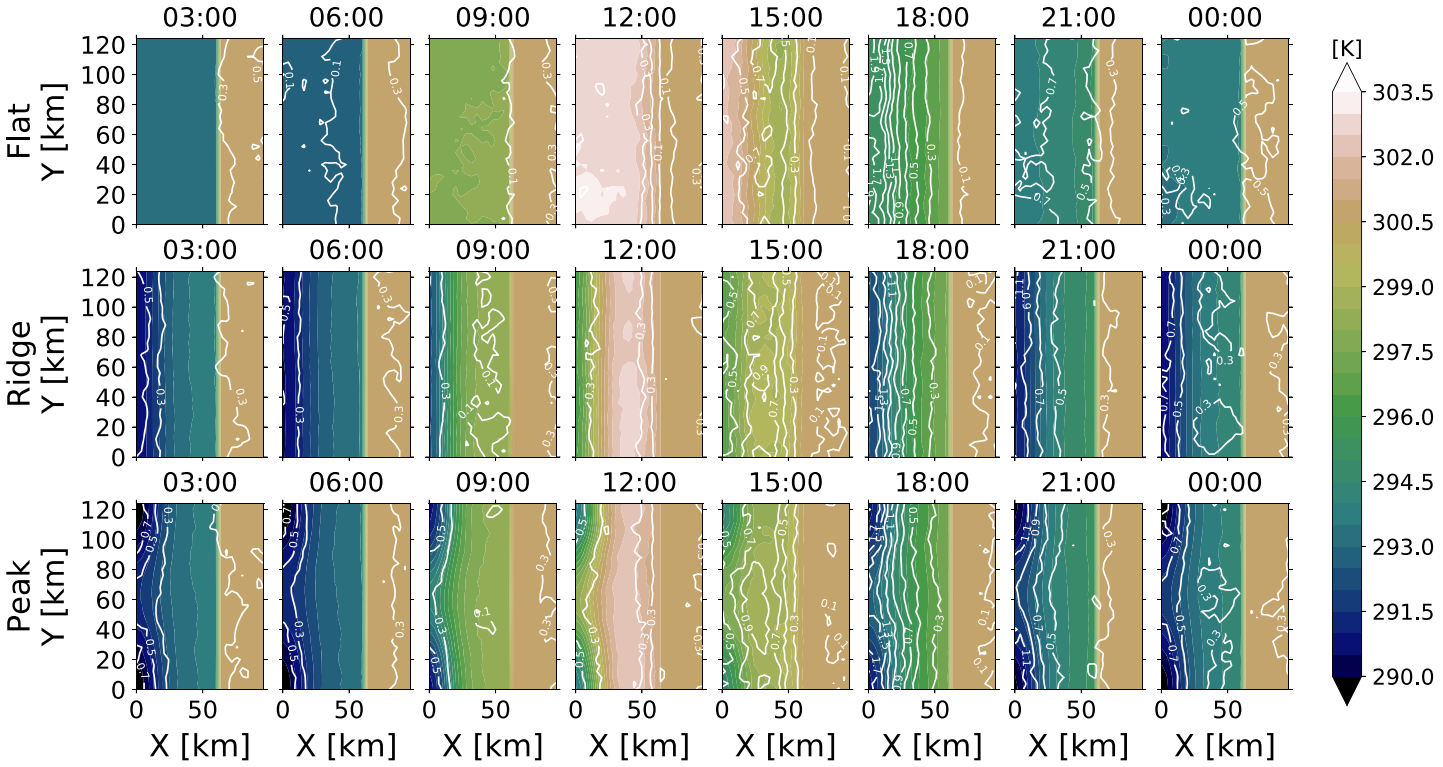

Figure 6. (first row) Surface temperature (shading) and cloud content, defined as the vertical integral of ice and water vapor over the troposphere (contours every 0.2 g/m^2, from 0.1 to 1.9 g/m^2) over the island and the coastal ocean every 3 hr, averaged over 200 days for simulation Flat. (second row) Same for simulation Ridge. (third row) Same for simulation Peak. The center of the island (where topography is) is on the left, at 0 km. The coastline is made visible by the sharp contrast between the sea surface temperature fixed at 301 K and the usually colder island.

topography are 0.6 K colder throughout the night and up to 2 K colder at midday and in the early afternoon (Figure 5b). The stronger diurnal warming in simulation Flat originates from both the difference in averaged height (1.3 K) and its reduced cloud shadowing of the surface (0.7 K). At night, the temperature difference is smaller than 1.3 K, probably because clouds' greenhouse effect decreases the energy loss of the surface in the simulations with topography.

The decreased warming during the day leads to a weaker sea breeze at the coast (Figure 2) and a smaller convective enhancement over the island (Figure 5a) even though precipitation is still larger on average with topography. The precipitation rate at 18:00 and 21:00 is roughly similar in all three simulations. But it is much more concentrated over the topography in simulations Ridge and Peak, and it persists through the night there.

To investigate whether this pattern occurs everyday and whether this influences the nocturnal offshore propagation, we investigate the difference between short and long propagation in the next section, similar to the analysis in Part I.

3.2. Difference Between Short and Long Propagation

We classify nocturnal propagation events based on the distribution of maximum distance of propagation from the coast (Figure 3) into quartiles as we did for simulation Flat in Part I. For the first quartile, nocturnal propagation does not extend further than 50 km from the coast in simulation Peak (Figure 7a) but, for the last quartile, we see long propagation as in simulation Flat, as well as the same convection pattern developing 100–150 km away from the coast around 22:00, similar to simulation Flat (see Part I): convection triggered far from the coast still occurs in the simulations with topography, even though it is less frequent and appears as a weaker signal in the composite (Figures 2b and 2c). For this quartile, there is little or no precipitation at night over the island (Figure 7b). Looking at the first and last quartiles for simulation Peak shows that gravity waves trigger offshore convection for long propagation (Figure 8b).

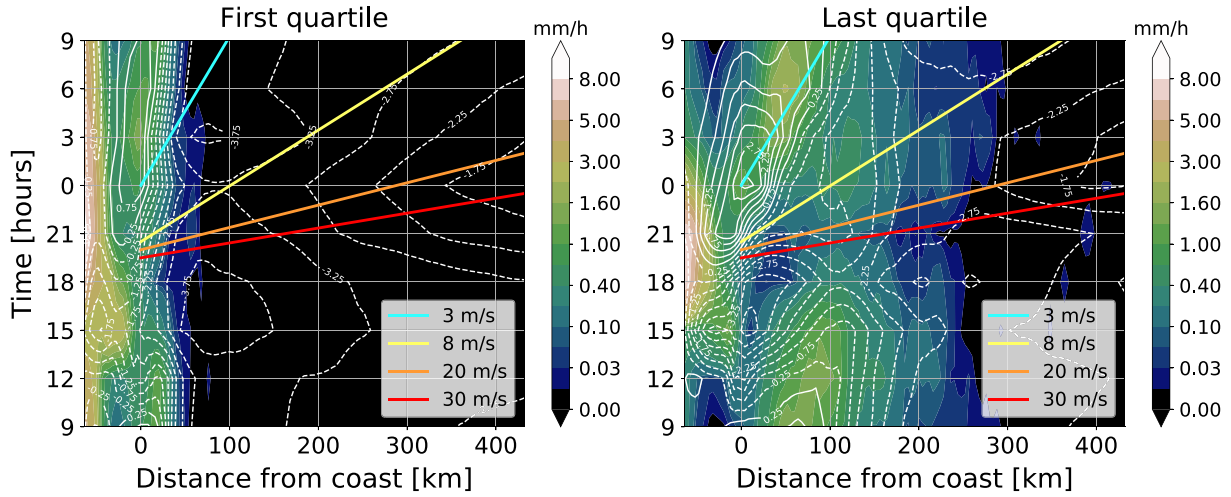

Figure 7. Diurnal composite of precipitation (shading) and wind at 75 m (contours, m/s) averaged over the days with (a) the shortest propagation and (b) the longest propagation of simulation Peak. The light blue, yellow, orange, and red lines indicate speeds of 3, 8, 20, and 30 m/s, respectively. In this case, the 25th percentile is at 50 km and the 75th percentile is at 142 km.

For the long propagation, this figure looks almost identical to the corresponding figure for simulation Flat (Figure 8 in Part I). The same gravity waves associated with the first and second baroclinic modes propagate at 30 and 20 m/s, respectively. Their cold phase triggers offshore convection (green line associated with convection in Figure 8b). Contrary to simulation Flat, no gravity wave is found for short propagation (Figure 8a).

Zoomed composites of the island and nearby ocean for long propagation days in all three simulations confirm that there is no convection in the morning over the island, even over topography, when long

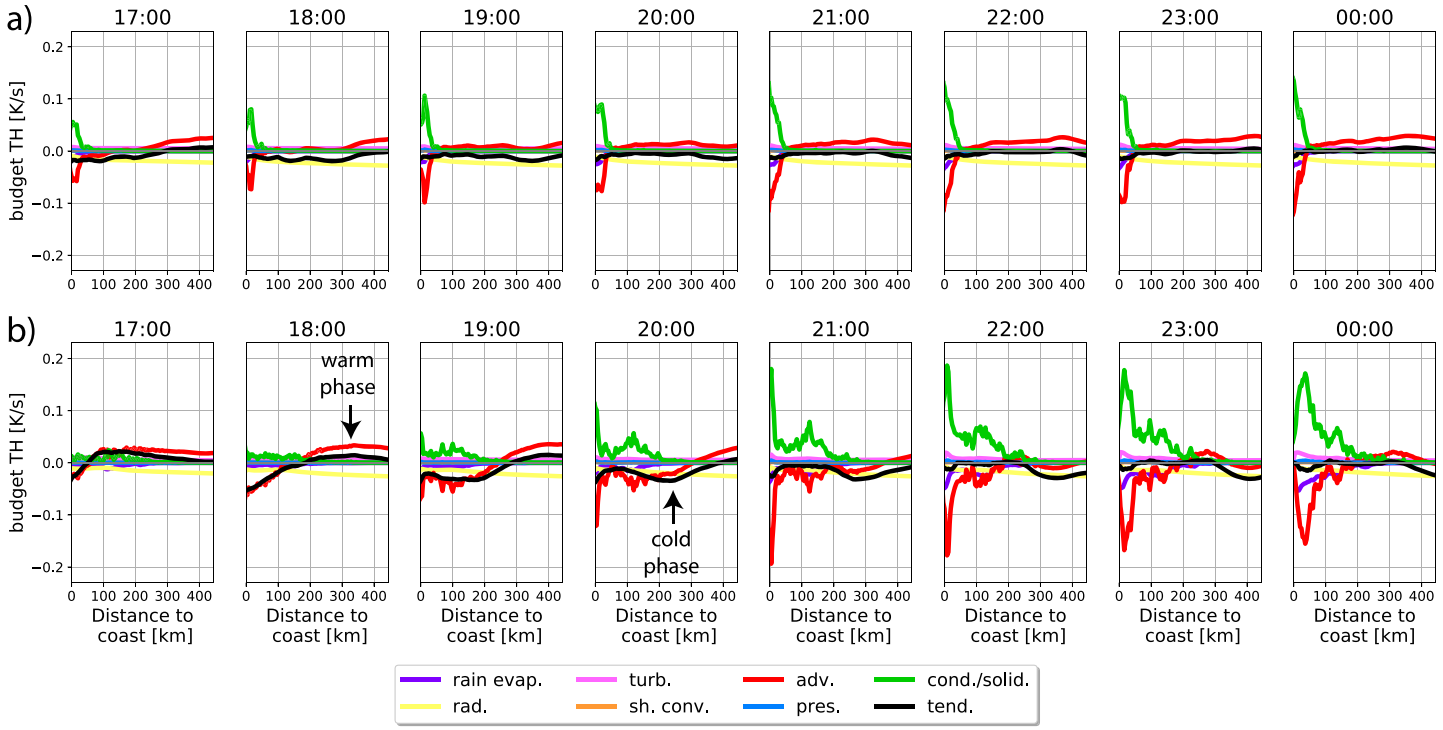

Figure 8. Transect of the 1-hr composites of the temperature budget between 17:00 and 00:00 at 4 km for (a) the first quartile of propagation and (b) the last quartile in simulation Peak. The island is on the left. The tendency, pressure, advection, shallow convection, turbulence, radiation, rain evaporation, and phase changes components are represented by the black, blue, red, orange, pink, yellow, purple, and green lines. Note that the abscissa starts at the coast and goes up to 400 km to be able to show the gravity wave.

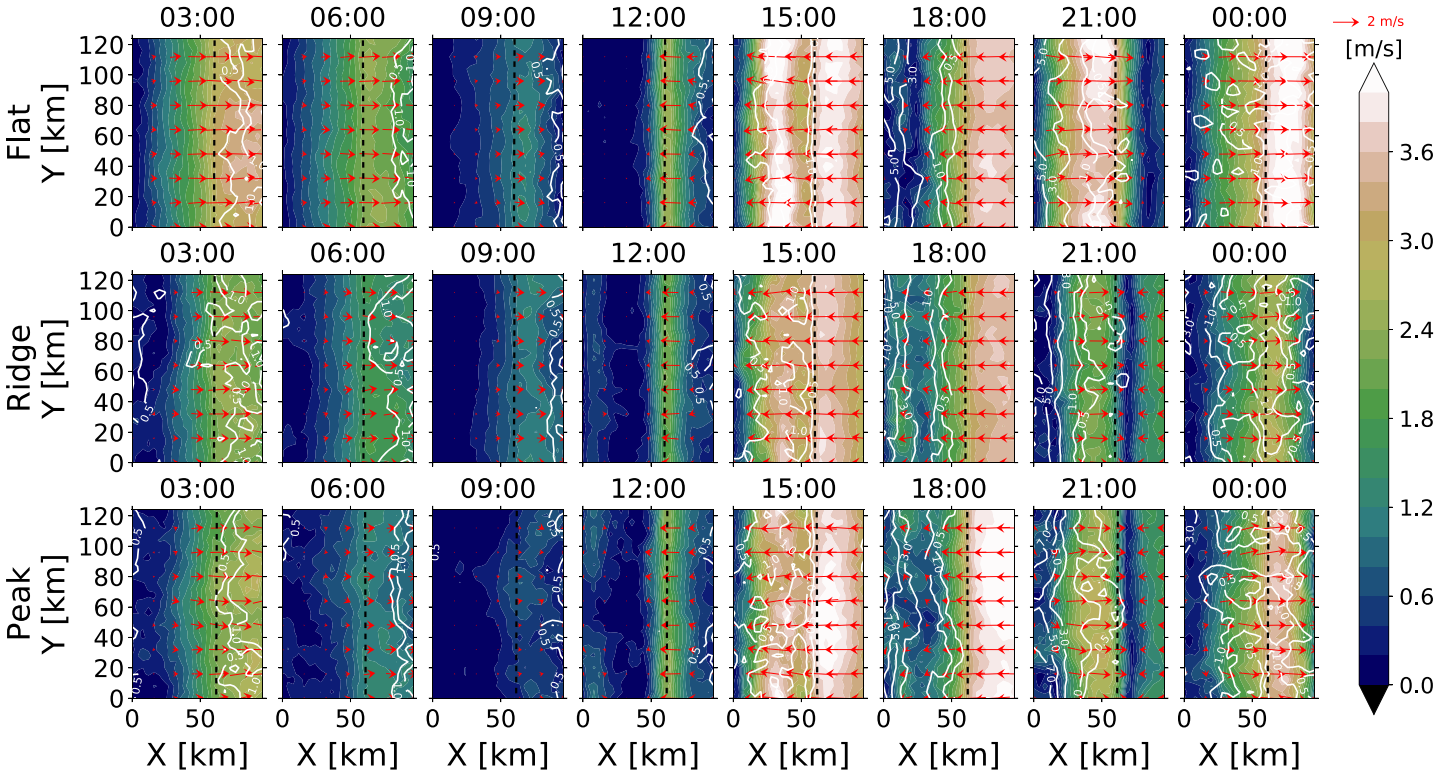

Figure 9. (first row) Wind (shading), wind direction (arrow), and precipitation (contours at 1, 2, 5, 10, 15, 20, and 25 mm/hr) over the island and the close ocean every 3 hr, for maximum propagation between 150 and 300 km over simulation Flat. (second row) Same for simulation Ridge. (third row) Same for simulation Peak. The center of the island is on the left, at 0 km. The black vertical dashed line represents the coast.

propagation occurs (Figure 9). Because the gravity waves necessary for offshore convection are triggered by the diurnal warming over land, they are only present for days when the cloud cover over the island is small in the morning. No gravity wave is emitted for short propagation probably because the heating increase in the afternoon is strongly reduced when convection stays over the island all day long. According to Figure 3, these days with short propagation and no fast gravity wave emitted in the afternoon are more frequent and explain why, on average, the diurnal hovmoller for simulations Ridge and Peak has convection all day long over the topography (Figures 2b and 2c).

3.3. Large-Scale Control of the Maximum Distance of Propagation

Similar to what happens in simulation Flat, the environmental conditions over the ocean, and more specifically the conditions at the top of the boundary layer, control the maximum distance of offshore propagation. For long propagation, once the top of the boundary layer is sufficiently deep, the cold phase of the fast gravity waves forced by the heating over land during the afternoon triggers convection far from the coast in both simulations with topography, as it did in simulation Flat (not shown). This allows convection to gradually propagate away from the island.

The picture is noticeably different when we consider propagation close to the coast (Figure 10). In order to compare with simulation Flat (Figure 11 first row from Part I), we only consider the first day of propagation between 0 and 80 km after days with propagation reaching further than 80 km from the coast; in particular, we discard cases where convection stays over the island on the same day or the day before. In simulation Peak (second row), the warm and dry anomaly advected at the top of the boundary layer prevents the development of convection far from the coast, which is reminiscent of what happens in simulation Flat. In simulation Ridge (first row), the advection of this dry anomaly is delayed and the anomaly itself is much smaller. These differences between simulations Ridge and Peak are investigated further in the next section.

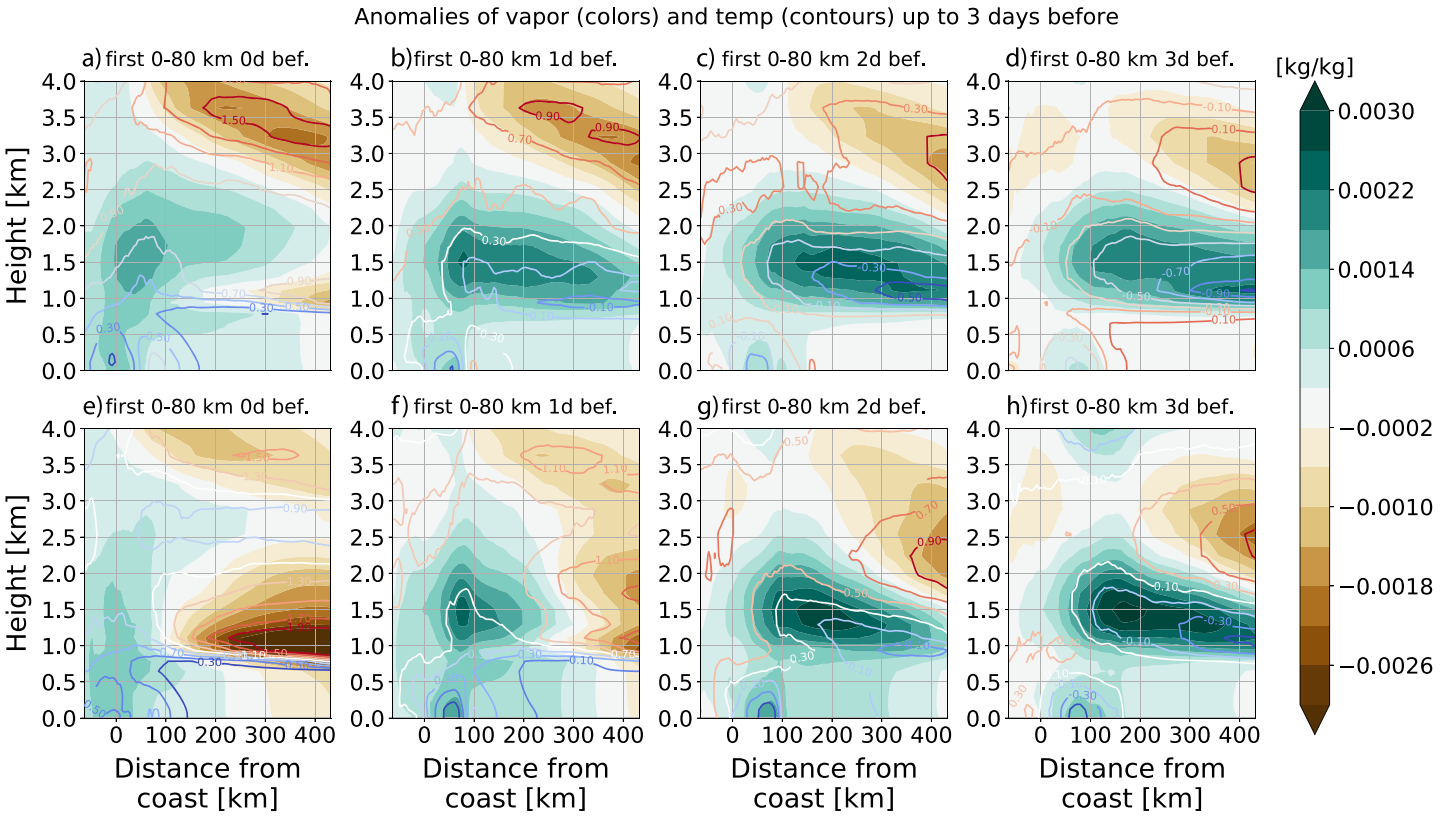

Figure 10. (first row) Daily-mean profiles of humidity (shading) and temperature (contours) anomalies in simulation Ridge for (a) the first day of propagation between 0 and 80 km, (b) 1 day before, (c) 2 days before, and (d) 3 days before. (second row) Same as first row for (e–h) simulation Peak. The anomalies are calculated relative to long-term averages over the 200 days of analysis.

4. Influence of the Shape of Topography

Both simulations with topography are more similar with each other in terms of convection over the island and offshore propagation of convection than either of them with simulation Flat, even though simulations Flat and Peak share some characteristics. In this section, we focus on the differences created by the shape of the island topography.

4.1. Mountain-Valley Breeze

Over the island, most changes in precipitation and wind patterns should result from the change in topography from a ridge to a peak and a pass. The first major difference occurs at 12:00 when the sea breeze starts to propagate over the island (Figure 9). Before convection appears over the mountains, upslope wind develops in both simulations with topography. But this upslope wind is doubled along the slopes of the peak (top and bottom of the domain, third row). At 15:00, the wind starts to diverge at the pass in simulation Peak while convection develops over the mountains in both simulations. At 18:00, a wind minimum appears at 40 km where the sea breeze and an outflow coming from the pass converge. This outflow is not present in simulation Ridge. At 21:00, convection is mainly localized over the highest topography, that is, along the ridge in simulation Ridge and over the peak in simulation Peak with a clear local minimum over the pass. The highest precipitation values found in simulation Peak over the topography are probably the signature of an ascent reinforced by the valley and may explain why precipitation is always larger over the island in simulation Peak relative to simulation Ridge (Figure 5a).

Wind going down the slopes of the peak converge in the pass, which results in an increased land breeze at the outflow of the pass. The land breeze is also stronger (1 m/s) on average in simulation Peak compared to simulation Ridge but is still 1 m/s weaker than the land breeze in simulation Flat. At 00:00 and 03:00, a slightly faster wind is still visible in the outflow from the valley in simulation Peak.

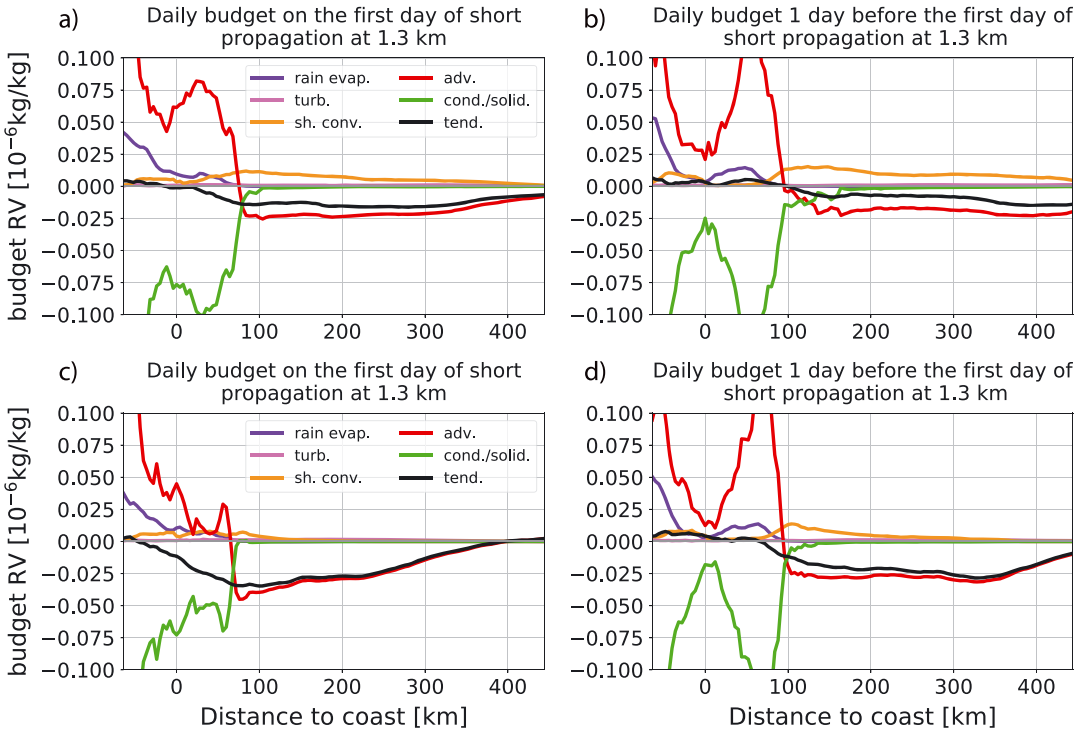

Figure 11. (first row) Transect of the daily budget of humidity at 1.3 km in simulation Ridge for (a) the first days of propagation between 0 and 80 km and (b) 1 day before. (second row) Same as first row in simulation Peak for (c) the first days of propagation between 0 and 80 km and (d) 1 day before.

Thus, the valley effect seems to reinforce the land breeze, especially in the outflow from the valley. But this reinforcement is not sufficient to exceed the speed of the land breeze in simulation Flat, probably because the stronger convergence near the center of the island in that case (see the wind 25 km from the center of the island at 15:00 in Figures 10a and 10c) leads to a larger convective enhancement, which in turn generates a stronger density current.

4.2. Impact on Large-Scale Control for Short Propagation

The main difference in distance of propagation between both simulations with topography occurs for intermediate distances of propagation, with simulation Peak having a higher proportion around 80 km similar to simulation Flat, while simulation Ridge have a smoother transition shifted toward longer propagation.

In the previous section, we mention that simulations Flat and Peak also have a very similar advection of warm and dry air prior to short propagation (Figure 10 from Part I and Figure 10). To investigate where this dry and warm anomaly originates from, we repeat the budget analysis done in Part I for the humidity at the top of the boundary layer. It shows that, in both simulations with topography, the advective term causes the drying (Figure 11). But this term and the tendency are larger in simulation Peak (bottom row) where the advection of the dry and warm anomaly also tends to inhibit shallow convection, which becomes much weaker than in simulation Ridge. This explains why the positive anomaly of humidity remains much larger for simulation Ridge in Figure 10 (first row). As in simulation Flat, the advection is mostly horizontal within 200 km from the coast (not shown).

To investigate how the shape of the topography can generate these different behaviors, we focus on the same days of short propagation as in Figures 10 and 11. But we look at both sides of the island to see how symmetric the circulation is relative to the island in all three simulations. To understand what is driving the advection of dry air observed as early as 2 days before in Figure 10, we focus on the symmetric and asymmetric parts of the circulation 3 days before the first short propagation (Figure 12). Because we select the distance of propagation from both sides of the island, all the days selected are arranged so that the short propagation happens on the right side of the island. The symmetric part is defined as the average of both

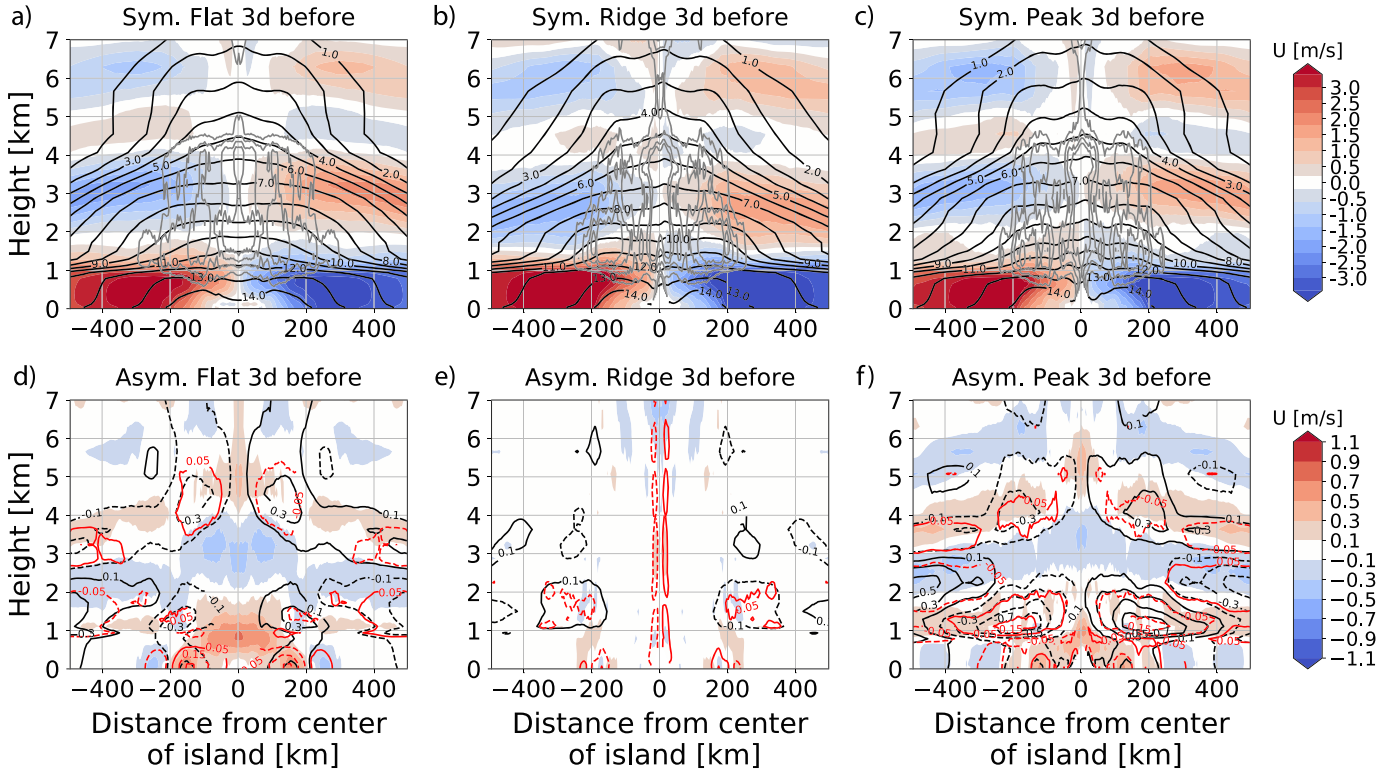

Figure 12. (first row) Symmetric component of the wind (shading), specific humidity (black contours, every g/kg), and specific cloud condensate (gray contours, every 10^{-5} kg/kg) 3 days before the first days of propagation between 0 and 80 km for simulations (a) Flat, (b) Ridge, and (c) Peak. (second row) Asymmetric component of the wind (shading), specific humidity (black contours, every 2×10^{-1} g/kg), and temperature (red contours, every 10^{-1} K) on the same day as the first row for the same simulations.

sides of the island. The asymmetric part is calculated as the difference between the original composite and the symmetric part.

In all three cases, the symmetric component is much larger than the asymmetric component indicating a strong forcing of the circulation by the island. The three simulations also have roughly similar wind and humidity patterns. On the other hand, the asymmetric component is much larger in simulations Flat and Peak than in simulation Ridge. In both cases, the wind and humidity patterns are very similar and highlight stronger convection around 200 km on the right side of the island, that is, where the dry anomaly will be advected later. An eastward wind associated with less convection on the left side of the island and the stronger convection on the right side is visible in the boundary layer around the island and is not stopped by the topography in simulation Peak. A westward anomaly between 1.5 and 3 km advects drier and warmer air from the right side of the domain. This lateral advection is mainly due to the shallow circulation generated by the asymmetric offshore convection. This shallow circulation also forces part of this anomaly to subside between 1 and 2 km as seen in Figures 10e–10h. There, it is advected toward the coast by the symmetric wind component and shuts down shallow convection on its way (Figures 11c and 11d).

Because this shallow circulation resulting from the asymmetric development of convection on one side of the island is totally absent from simulation Ridge (Figure 12e), the dry and warm anomaly located at an altitude of 3 km, 400 km from the coast 3 days before the short propagation does not subside (Figures 10a–10d). Thus, the onshore wind at the top of the boundary layer does not advect an anomaly as dry as in simulations Peak and Flat.

Even though simulations Ridge and Peak behave very similarly in many respects, their mountain shapes generate some key differences for days with short propagation. The mountain ridge prevents the development of a strong asymmetric convective pattern, permitted by the pass in simulation Peak. In addition to preventing the mean flow from crossing the mountain range, the main effect of the ridge seems to force

convection always over the mountain range, generating an upward transport over the island and a more symmetric circulation.

In simulation Peak (as well as simulation Flat), the asymmetry is responsible for the advection of a much drier and warmer anomaly on top of the boundary layer. This anomaly forces convection to stay close to the coast longer than in simulation Ridge where it can be quickly eroded and allows for longer propagation much sooner.

5. Discussion and Conclusion

In this paper, we investigate how topography affects the nocturnal offshore propagation of convection around an idealized tropical island and how the shape of the island topography (idealized mountain ranges represented by a ridge or a peak with a pass) modulates it in the Radiative Convective Equilibrium version of the mesoscale nonhydrostatic atmospheric model Meso-NH.

Adding a mountain range on the island significantly decreases the surface temperature above the island. It also affects the pattern of convection and its offshore propagation relative to a simulation with a flat Island (simulation Flat):

- On average, convection stays over the highest topography at the center of the island at night in both simulations with topography, resulting in an increased cloud cover and precipitation at night and in the morning. The presence of these clouds reduces the average surface temperature difference between simulation Flat and both simulations with topography, probably due to the greenhouse effect of clouds. During the day, they have an opposite effect as they reduce the diurnal warming over land.
- The average propagation speed of the land breeze is much smaller because of the weaker land breeze circulation and the competing effect of convection maintained over the mountains at night. However, this speed increases on days when convection is not maintained over the island at night. The weaker land breeze is also responsible for a reduced maximum distance of propagation, with convection anchored 25% of the days on the island or within 50 km of the coast.
- For long-propagation days, the same gravity waves as in simulation Flat are found. The first and second baroclinic modes propagating, respectively, at 30 and 20 m/s trigger offshore convection, while the higher-order modes play a role in reinforcing existing convection prior to the land breeze front. Because clouds stay over the island all day during short propagation days, these gravity waves are only seen for long propagation.

The two simulations with topography are very similar, indicating that the shape of the mountain has little impact on the land-sea breeze circulation. However, two distinct features have a notable impact on convection and its propagation:

- The valley seems to reinforce convection as the highest precipitation value occurs over the peak and on average in simulation Peak, as was emphasized by J.-H. Qian (2008). But it does not change the timing of precipitation. This valley also generates land-valley breezes visible in the outflow of the valley. These winds reinforce the offshore wind relative to simulation Ridge. But this reinforcement, also mentioned by Vincent and Lane (2016), does not compensate the decrease in land breeze speed caused by convection staying over the topography later in the evening if not all night long. We do not see any katabatic wind. But in our cases where convection clings to the island at night, these winds would most likely be compensated by the weaker land breeze.
- The ridge, even though its height does not correspond to a Froude number above one, acts as a much stronger barrier than the peak and pass. Momentum reaching the island below 600 m is transported vertically and forces the large-scale circulation to be much more symmetric in simulation Ridge. In simulation Peak, the lower pass allows the flow to propagate more easily across the island. This creates situations when offshore convection is much stronger on one side of the island while suppressed on the other side. The stronger offshore convection generates a local circulation that advects drier and warmer air between 1.5 and 3 km from the sides of the domain. As this anomaly subsides, it is advected onshore and above the boundary layer by the symmetric component of the large-scale circulation. Along its way, it suppresses shallow convection and forces convection to stay close to the coast. The larger and more stable anomaly takes longer to be removed by shallow convection than the weaker anomaly advected in simulation

Ridge. In the latter, shallow convection rapidly deepens the boundary layer and reduces convective inhibition, allowing convection to gradually propagate further away from the coast every day. This explains why the distribution of distance of propagation is much smoother for simulation Ridge.

Simulations Peak and Flat have the same distribution of distance of propagation and the same warm and dry anomaly much closer to the coast for the short propagation cases. In fact, this anomaly is even stronger and close to the coast for simulation Flat because there is no mountain range to act as a barrier on the mean flow, leading to a larger asymmetry. This shows that a small change in topography can significantly affect the offshore propagation of convection near the island.

The results presented in this study confirm those from Part I and might explain the relationship between convection over islands and the propagation of the MJO over the Maritime Continent. The gradual enhancement of the diurnal cycle over islands followed by an enhancement over the surrounding oceans prior to the MJO envelope could very well work in the same way as the gradual offshore propagation of convection that we observe in our simulations and create an environment favorable for the MJO envelope to propagate over the oceans. Similarities with Phases 4 and 5 of the MJO when the envelope is over the Maritime Continent are less obvious, partly because these phases are characterized by sustained convection over the ocean, a usually weaker diurnal cycle over the island and a strong large-scale forcing, which we do not study in our simulations without large-scale wind forcing. It is nonetheless noteworthy that, in our simulations, days with short propagation have clouds over the topography all day long and a weaker land-sea breeze circulation. The oceanic moisture supply being higher during such days than in cases with strong diurnal cycle over land, this might relate to the weakened barrier effect of the islands for the propagation of the MJO when their diurnal cycle is weakened. Finally, it is possible that dry and warm air advected during the last phases of the MJO suppresses the diurnal cycle over both ocean and island, the same way as the dry and warm anomaly in the lower troposphere forces convection to stay near the coast and reduces the diurnal cycle over land.

Several steps are still needed to bridge the gap between our ideal experiments and reality. Considering how a simple change of topography can modify the offshore propagation of convection in our simulations, one possibility would be to study the effect of topography for different heights as several islands of the Maritime Continent have mountain ranges higher than what we modeled, as well as more realistic island topography. Another extension of this work would be to assess the impact of the mean flow on the propagation mechanisms.

Acknowledgments
We thank two anonymous reviewers for their helpful comments. We acknowledge the financial support of the Glavish Postdoctoral Fellowship and the Buckley-Glavish Lectureship, as well as support from the University of Auckland. We also wish to acknowledge the use of New Zealand eScience Infrastructure (NeSI) high-performance computing facilities and consulting support as part of this research. New Zealand's national facilities are provided by NeSI and funded jointly by NeSI's collaborator institutions and through the Ministry of Business, Innovation and Employment's Research Infrastructure programme (https://www.nesi.org.nz). We also thank MesoNH team at CNRM and LA, Toulouse, France: Christine Lac, Juan Escobar, Gaelle Gautier, Philippe Vautelet, as well as Stéphanie Faroux, Jean-Pierre Pinty, and Jean-Pierre Chaboureau. Data used in this study can be found here: (https://www.dropbox.com/sh/gyt8uruv2f36cer/AAB0uE_9qeyOPqaRnBg5Gfv_a?dl=0).

References

Coppin, D., & Bellon, G. (2019). Physical mechanisms controlling the offshore propagation of convection in the tropics: 1. Flat island. *Journal of Advances in Modeling Earth Systems*, *11*, 3042–3056. https://doi.org/10.1029/2019MS001793

Hagos, S. M., Zhang, C., Feng, Z., Burleyson, C. D., De Mott, C., Kerns, B., et al. (2016). The impact of the diurnal cycle on the propagation of Madden-Julian Oscillation convection across the Maritime Continent. *Journal of Advances in Modeling Earth Systems*, *8*, 1552–1564. https://doi.org/10.1002/2016MS000725

Hassim, M. E. E., Lane, T. P., & Grabowski, W. W. (2016). The diurnal cycle of rainfall over New Guinea in convection-permitting WRF simulations. *Atmospheric Chemistry and Physics*, *16*(1), 161–175.

Ichikawa, H., & Yasunari, T. (2007). Propagating diurnal disturbances embedded in the Madden-Julian Oscillation. *Geophysical Research Letters*, *34*, L18811. https://doi.org/10.1029/2007GL030480

Ichikawa, H., & Yasunari, T. (2008). Intraseasonal variability in diurnal rainfall over New Guinea and the surrounding oceans during austral summer. *Journal of Climate*, *21*, 2852–2868.

Lac, C., Masson, V., Aouizerats, B., Augros, C., Aumond, P., Caumont, O., et al. (2018). Overview of the Meso-NH model version 5.4 and its applications. *Geoscientific Model Development*, *11*, 1929–1969.

Lafore, J. P., Stein, J., Asencio, N., Bougeault, P., Ducrocq, V., Duron, J., et al. (1998). The Meso-NH atmospheric simulation system. Part I: Adiabatic formulation and control simulations. *Annals of Geophysics*, *16*, 90–109.

Love, B. S., Matthews, A. J., & Lister, G. M. S. (2011). The diurnal cycle of precipitation over the Maritime Continent in a high-resolution atmospheric model. *Quarterly Journal of the Royal Meteorological Society*, *137*, 934–947.

Madden, R. A., & Julian, P. R. (1971). Detection of a 40-50 day oscillation in the zonal wind in the Tropical Pacific. *Journal of the Atmospheric Sciences*, *28*, 702–708. https://doi.org/10.1175/1520-0469(1971)028<0702:DOADOI>2.0.CO;2

Madden, R. A., & Julian, P. R. (1972). Description of global-scale circulation cells in the tropics with a 40–50 day period. *Journal of the Atmospheric Sciences*, *29*(6), 1109–1123. https://doi.org/10.1175/1520-0469(1972)029<1109:DOGSCC>2.0.CO;2

Madden, R. A., & Julian, P. R. (1994). Observations of the 40-50-Day tropical oscillation—A review. *Monthly Weather Review*, *122*, 814–837. https://doi.org/10.1175/1520-0493(1994)122<0814:OOTDTO>2.0.CO;2

Mapes, B. E., Warner, T. T., & Xu, M. (2003). Diurnal patterns of rainfall in Northwestern South America. Part III: Diurnal gravity waves and nocturnal convection offshore. *Monthly Weather Review*, *131*, 830–844.

Masson, V., Le Moigne, P., Martin, E., Faroux, S., Alias, A., Alkama, R., et al. (2013). The SURFEXv7.2 land and ocean surface platform for coupled or offline simulation of Earth surface variables and fluxes. *Geoscientific Model Development*, *6*(4), 929–960.

Mori, S., Hamada, J.-I., Sakurai, N., Fudeyasu, H., Kawashima, M., Hashiguchi, H., et al. (2011). Convective systems developed along the coastline of Sumatera Island, Indonesia, observed with an X-band Doppler radar during the HARIMAU2006 campaign. *Journal of the Meteorological Society of Japan*, *89A*, 61–81.

Mori, S., Hamada, J. I., Tauhid, Y. I., & Yamanaka, M. D. (2004). Diurnal land-sea rainfall peak migration over Sumatra Island, Indonesian Maritime Continent, observed by TRMM Satellite and Intensive Rawinsonde Soundings. *Monthaly Weather Review*, *132*, 2021–2039.

Neale, R., & Slingo, J. (2003). The Maritime Continent and its role in the global climate: A GCM study. *Journal of Climate*, *16*(5), 834–848.

Peatman, S. C., Matthews, A. J., & Stevens, D. P. (2014). Propagation of the Madden-Julian Oscillation through the Maritime Continent and scale interaction with the diurnal cycle of precipitation. *Quarterly Journal of the Royal Meteorological Society*, *140*, 814–825.

Peatman, S. C., Matthews, A. J., & Stevens, D. P. (2015). Propagation of the Madden-Julian Oscillation and scale interaction with the diurnal cycle in a high-resolution GCM. *Climate Dynamics*, *45*, 2901–2918.

Qian, J.-H. (2008). Why precipitation is mostly concentrated over islands in the Maritime Continent. *Journal of the Atmospheric Sciences*, *65*, 1428–1441. https://doi.org/10.1175/2007JAS2422.1

Qian, T., Epifanio, C. C., & Zhang, F. (2012). Topographic effects on the tropical land and sea breeze. *Journal of the Atmospheric Sciences*, *69*, 130–149.

Qian, J.-H., Robertson, A. W., & Moron, V. (2013). Diurnal cycle in different weather regimes and rainfall variability over Borneo associated with ENSO. *Journal of Climate*, *26*, 1772–1791.

Vincent, C. L., & Lane, T. P. (2016). Evolution of the diurnal precipitation cycle with the passage of a Madden-Julian Oscillation event through the Maritime Continent. *Monthly Weather Review*, *144*, 1983–2005.

Yang, G., & Slingo, J. (2001). The diurnal cycle in the tropics. *Monthly Weather Review*, *129*, 784–801.

Yokoi, S., Mori, S., Katsumata, M., Geng, B., Yasunaga, K., Syamsudin, F., et al. (2017). Diurnal cycle of precipitation observed in the western coastal area of Sumatra Island: Offshore preconditioning by gravity waves. *Monthly Weather Review*, *145*, 3745–3761.

Zhang, C. U. o. M. (2005). Madden Julian Oscillation. *Reviews of Geophysics*, *43*, RG2003. https://doi.org/10.1029/2004RG000158